

PHYSICAL REVIEW D

PARTICLES AND FIELDS

THIRD SERIES, VOLUME 42, NUMBER 7

1 OCTOBER 1990

Test of QED to fourth order by study of four-lepton final states in e^+e^- interactions at 29 GeV with the Mark II detector

M. Petradza, ^{γ , (r)} R. Thun, ^{γ} G. Abrams, ^{α} D. Amidei, ^{α , (h)} A. R. Baden, ^{α , (m)} T. Barklow, ^{δ}
A. Boyarski, ^{δ} J. Boyer, ^{α} P. R. Burchat, ^{δ , (g)} D. L. Burke, ^{δ} F. Butler, ^{α , (p)} J. M. Dorfan, ^{δ} G. J. Feldman, ^{δ}
G. Gidal, ^{α} L. Gladney, ^{δ , (q)} M. S. Gold, ^{α} G. Goldhaber, ^{α} J. Haggerty, ^{α , (a)} G. Hanson, ^{δ} K. Hayes, ^{δ}
D. Herrup, ^{α , (k)} T. Himel, ^{δ} R. J. Hollebeek, ^{δ , (q)} W. R. Innes, ^{δ} J. A. Jaros, ^{δ} J. A. Kadyk, ^{α} D. Karlen, ^{δ , (c)}
S. R. Klein, ^{δ , (b)} A. J. Lankford, ^{δ} R. R. Larsen, ^{δ} B. W. LeClaire, ^{δ , (s)} M. E. Levi, ^{δ , (o)} N. S. Lockyer, ^{δ , (q)}
V. Lüth, ^{δ} M. E. Nelson, ^{α , (d)} R. A. Ong, ^{δ , (h)} M. L. Perl, ^{δ} B. Richter, ^{δ} K. Riles, ^{δ , (f)} P. C. Rowson, ^{α , (i)}
T. Schaad, ^{β , (l)} H. Schellman, ^{α , (k)} W. B. Schmidke, ^{α} P. D. Sheldon, ^{α , (n)} G. H. Trilling, ^{α} D. R. Wood, ^{α , (e)}
and J. M. Yelton, ^{δ , (j)}

^{α} Lawrence Berkeley Laboratory and Department of Physics, University of California, Berkeley, California 94720

^{β} Harvard University, Cambridge, Massachusetts 02138

^{γ} University of Michigan, Ann Arbor, Michigan 48109

^{δ} Stanford Linear Accelerator Center, Stanford University, Stanford, California 94309

(Received 26 March 1990)

We have tested QED to fourth order in the coupling constant α in the large- Q^2 region by studying four-lepton final states in e^+e^- interactions with the Mark II detector at the SLAC storage ring PEP ($\sqrt{s}=29$ GeV). All four final-state particles were detected at large angles with respect to the beam axis. For an integrated luminosity of 205 pb^{-1} , we observed ten $e^+e^-e^+e^-$, ten $e^+e^-\mu^+\mu^-$, and one $\mu^+\mu^-\mu^+\mu^-$ events with opposite-charge pair masses greater than $1 \text{ GeV}/c^2$. These events show good agreement with the complete α^4 QED calculation.

I. INTRODUCTION

We report a test of QED to fourth order in the coupling constant α with data taken with the Mark II detector at the SLAC storage ring PEP. We have measured and compared with theory the following processes:

$$e^+e^- \rightarrow e^+e^-e^+e^- ,$$

$$e^+e^- \rightarrow e^+e^-\mu^+\mu^- ,$$

$$e^+e^- \rightarrow \mu^+\mu^-\mu^+\mu^- .$$

The cross section for these processes is very small (of the order of a tenth of a picobarn), in the region of large opposite-charge pair masses and large scattering angles. In this region the background to four-lepton processes is small, making them easily distinguishable, despite the smallness of the cross section.

The motivation of this analysis is the following: QED is the physical theory best established experimentally. It serves as the prototype of more evolved theories, such as the electroweak theory and QCD. The degree of precision attained in the measurements and predictions of

$g-2$ for the electron¹ and the muon² severely constrain the existence of new physics³ (composite leptons, excited leptons, supersymmetric particles, etc.) at small Q^2 and in higher-order QED. The nonobservation of significant deviations from the theory in measurements of the differential cross sections of Bhabha scattering and muon-pair production establish QED to order α^2 and α^3 at small distances. The results reported here extend tests of QED to higher order (α^4) at large Q^2 . By requiring all leptons to be detected one accomplishes two things. First, at large angles, virtual bremsstrahlung processes are expected to dominate and the production of two virtual photons becomes measurable. Second, if massive new particles decaying into leptons are produced, an excess of events would appear above the QED prediction.

The proliferation of Feynman diagrams with increasing order make the calculations of QED contributions in order α^4 quite difficult [the Bhabha scattering reaction (α^2) involves 2 Feynman diagrams, radiative Bhabha scattering involves 8, but final states with 4 electrons from e^+e^- interactions involve 36]. A Monte Carlo program, where all Feynman diagrams contributing to lowest order are taken into account, was written by Berends *et al.*⁴ to

generate the four-body final states. This is the one used in this analysis for comparison with the data.

In the past, other collaborations⁵ have made similar measurements at center-of-mass energies ranging from 14 to 47 GeV and found good agreement between data and QED predictions to α^4 . One group⁶ initially found some disagreement but recently reported agreement⁷ between their data and the Monte Carlo program of Berends *et al.*⁴

II. THEORETICAL DESCRIPTION

The Feynman diagrams which describe four-lepton final states always contain two photon propagators and one lepton propagator. They can be classified into four groups⁴ as follows.

Group (I) is the “bremsstrahlung” group [shown in Fig. 1(a)], where one of the photons has a positive four-momentum squared $Q^2 > 0$ (timelike), and the other has $Q^2 < 0$. They are most important in the reactions examined in this paper.

The “annihilation” (II) and “conversion” (III) groups are shown in Figs. 1(b) and 1(c), respectively. Both photons satisfy $Q^2 > 0$. They can be neglected as soon as one of the electrons is emitted at small angles. However, they

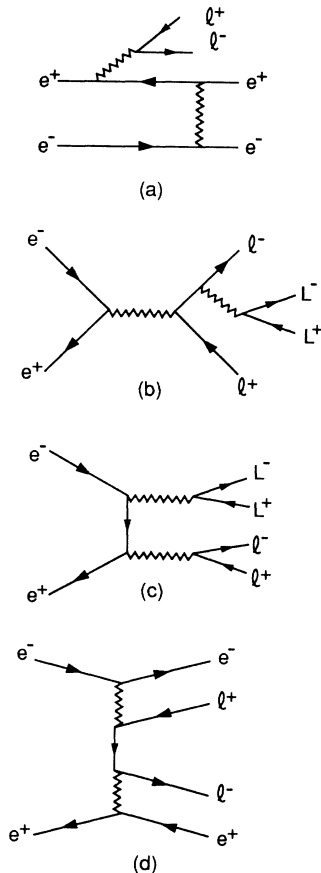


FIG. 1. Diagrams contributing to four-lepton final states; an example from the (a) bremsstrahlung; (b) annihilation; (c) conversion; and (d) multiperipheral groups.

contribute significantly in the reactions $e^+e^-e^+e^-$, $e^+e^-\mu^+\mu^-$, and $\mu^+\mu^-\mu^+\mu^-$ when all leptons are emitted at large angles.

Group (IV) is the “multiperipheral” group [shown in Fig. 1(d)], where both photons satisfy $Q^2 < 0$. Of the four classes, the multiperipheral group contributes the least to the four-lepton final states in this study.

III. ANALYSIS

A. Event selection

The analyzed data were taken with the Mark II detector at the PEP e^+e^- storage ring ($\sqrt{s}=29$ GeV), and corresponded to an integrated luminosity of 205 ± 3 pb⁻¹ as determined from Bhabha events. The Mark II detector, shown in Fig. 2, has been described elsewhere⁸ and we briefly present here the elements essential to this analysis. A 16-layer cylindrical drift chamber (DC) and a 7-layer precision vertex drift chamber (VC) provided charged particle tracking in a 2.3-kG solenoidal magnetic field over $\sim 85\%$ of the solid angle. Electrons (e^\pm) were detected by a lead-liquid-argon calorimeter covering $|\cos\theta| \leq 0.7$. Muons (μ^\pm) were detected in the central region by a four-layer hadron-absorber-proportional-wire-chamber system covering $\sim 55\%$ of the solid angle. In addition we used an end-cap (EC) shower counter⁹ to distinguish electrons from muons in the angular range $0.76 \leq |\cos\theta| \leq 0.85$.

We present two analyses which differ in the requirement placed on the invariant mass of any oppositely charged pair of tracks. Both cases were examined in view of our goal of testing QED at small distances (or high Q^2). In case (A) each event was required to satisfy the following criteria.

(1) It must contain four *good* charged tracks with zero net total charge. A *good* track had a momentum of at least 0.5 GeV/c, passed sufficiently close to the interaction point ($r \leq 0.05$ m, $z \leq 0.1$ m), through at least 6 DC and 3 VC layers, and had a χ^2 per degree of freedom of at most 10.

(2) At least two tracks should be in the barrel of the detector, $135^\circ > \theta > 45^\circ$, where θ is the angle with respect to the beam direction. This condition was imposed because the Mark II trigger required at least two tracks in this angular region in the absence of a significant calorimeter signal. The other tracks could be at any angle in the interval $152^\circ > \theta > 28^\circ$.

(3) The energy of an event, which was approximated by the scalar sum of the charged-particle momenta, $P_s \equiv \sum_{i=1,4} |P_i|$, should be at least 20 and not more than 40 GeV. Initial- or final-state radiation produces events with $P_s < 29$ GeV. Collinear initial-state radiation is not visible in the detector, but affects the observed cross section. Final-state radiation is, in principle, visible in the detector. The upper limit of 40 GeV on P_s is well above the c.m. energy of 29 GeV (intrinsic momentum resolution $\delta p/p = 0.01p$, with p in GeV/c) and helps reject cosmic rays and mistracked events.

(4) All pairs of tracks with zero net charge must have an invariant mass of at least 1 GeV/c². This cut helps

reduce the backgrounds from hadronic resonance production and from single-photon conversion in the detector material to an e^+e^- pair.

(5) In each event there should be at least three identified leptons, or two identified leptons of the same charge sign. An identified lepton must have a momentum of at least 1 GeV/c in order to minimize hadronic misidentification. We used rather loose identification criteria for leptons, taking advantage of the low backgrounds. These identification criteria are the following.

(a) Electron candidates in the liquid-argon (LA) calorimeter must satisfy shower development criteria expected for an electromagnetic cascade. Also the energy E measured in the LA calorimeter and the momentum P measured with the drift chamber must be compatible.¹⁰ This requirement is essentially equivalent to an $E/P > 0.6$. In the end-cap shower counter, a candidate electron must have a momentum of at least 3 GeV/c and $E/P > 0.5$.

(b) Muon candidates are required to leave hits in the layers of the muon system consistent with the expected range and track extrapolation error. A real muon would have to scatter in position or momentum by more than 3 standard deviations to avoid being detected using this criterion.¹⁰

When only three leptons are identified in an event, the fourth track is assumed to conserve lepton number. Similarly, in events with two identified leptons of the same sign, the identities of the other two tracks are also fixed by the assumption of lepton-number conservation. We checked that the assignment inferred from the assumption of lepton-number conservation is consistent with that made by our identification algorithm for those tracks that were not explicitly identified as leptons. There were no inconsistencies in the data.

Thirty-nine events passed all kinematical cuts (1–4). Particle identities could be determined in 21 of these events. Ten were identified as $e^+e^-e^+e^-$, ten as $e^+e^-\mu^+\mu^-$, and one as $\mu^+\mu^-\mu^+\mu^-$. The main reason for failing to identify four-lepton events was the finite coverage of the electromagnetic calorimeters and of the muon identification system.

Case (B) was basically a check of the stability of our results under kinematical cuts less severe than the pair mass cut of 1 GeV/c². The cuts used in case (B) were identical to those of case (A), except for cut 4, which in case (B) required that all pairs of tracks have an invariant mass of at least 0.6 GeV/c². An additional kinematical cut used in case (B) to reduce background coming from τ decays, did not affect at all the results of case (A). This additional cut demanded that the invariant mass of any three tracks be at least 1.6 GeV/c². Twenty-eight events were identified: 14 as $e^+e^-e^+e^-$, 13 as $e^+e^-\mu^+\mu^-$, and 1 as $\mu^+\mu^-\mu^+\mu^-$. Thirty-seven events did not meet the identification criteria for reasons similar to those in case (A).

B. Background estimation

The reactions which can *a priori* contribute as background to the examined processes are

$$\begin{aligned} e^+e^- &\rightarrow e^+e^-\tau^+\tau^-, \\ e^+e^- &\rightarrow e^+e^-h^+h^-, \\ e^+e^- &\rightarrow \tau^+\tau^-, \\ e^+e^- &\rightarrow q\bar{q} \rightarrow \text{hadrons}, \\ e^+e^- &\rightarrow e^+e^-\gamma\gamma. \end{aligned}$$

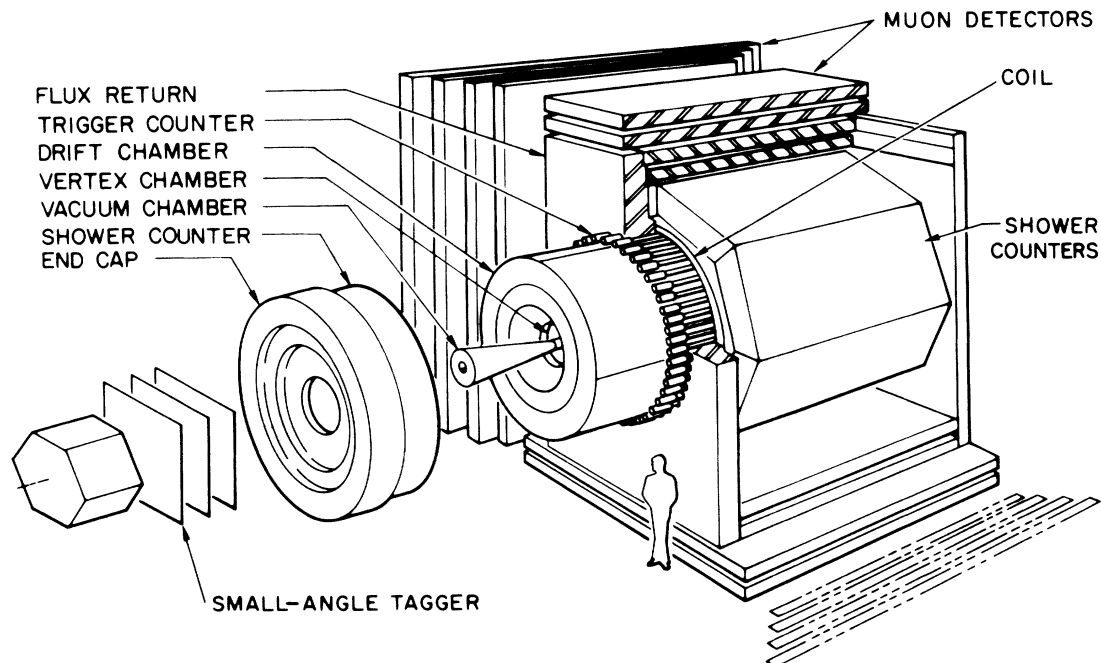


FIG. 2. The Mark II detector at PEP.

The most important source of potential background is $e^+e^- \rightarrow e^+e^-\tau^+\tau^-$, since both τ 's may decay into a charged lepton (an electron or a muon) plus neutrinos. Events from this reaction were simulated using the Monte Carlo calculation of Berends *et al.*⁴ The generated events corresponded to an integrated luminosity of $10\,055\text{ pb}^{-1}$.

The background from $e^+e^- \rightarrow e^+e^-h^+h^-$, where h is a hadron, was determined from simulated events using the same Monte Carlo programs of Berends *et al.*⁴ to generate $e^+e^- \rightarrow e^+e^-q\bar{q}$ events. The Lund Monte Carlo code¹¹ was used to fragment the quarks into hadrons. The generated events corresponded to an integrated luminosity of 5156 pb^{-1} .

The reaction $e^+e^- \rightarrow \tau^+\tau^-$ contributes as a background when one τ decays into an electron or muon plus neutrinos and the other τ decays into charged and neutral pions plus a neutrino, where the pions are misidentified as electrons or muons. The generated events corresponded to an integrated luminosity of 512 pb^{-1} .

The process $e^+e^- \rightarrow q\bar{q} \rightarrow \text{hadrons}$ may contribute through the decay of a hadron to an electron or muon, or through the misidentification of a hadron as an electron or muon. The Lund Monte Carlo code with Lund and Peterson¹² fragmentation methods was used to generate events corresponding to an integrated luminosity of 627 pb^{-1} .

Higher-order radiative Bhabha events $e^+e^- \rightarrow e^+e^-\gamma\gamma$ can fake $e^+e^-e^+e^-$ events if the radiated photons convert in the beam pipe, producing electrons.

Because of the smallness of its cross section, this process is expected to contribute minimally to the background at the high- Q^2 regions examined in this study. A Monte Carlo generator¹³ was used to reproduce events corresponding to an integrated luminosity of 655 pb^{-1} .

As shown in Table I the backgrounds expected from these various processes are found to be small compared to the four-lepton signal.

C. Comparison with QED

The Monte Carlo event generator⁴ which was used to obtain the results presented in this analysis was especially designed to describe four-lepton processes where all four leptons are emitted at large angles. All Feynman diagrams contributing to fourth order were taken into account. They included all possible virtual photon and Z^0 exchanges to fourth order, although the latter ones were estimated to make a negligible contribution at a center-of-mass energy of 29 GeV . All the kinematic cuts used for the generation of the four-lepton final states, extended a few standard deviations beyond the final acceptance criteria. These kinematical requirements were as follows.

(a) The scattering angle of the final-state leptons was required to be within the angular interval $20^\circ \leq \theta \leq 160^\circ$ with respect to the beams.

(b) All leptons were required to have a momentum of at least $0.1\text{ GeV}/c$.

(c) All oppositely charged-lepton pair combinations were required to have an invariant mass of at least 0.5

TABLE I. Number of observed and expected signal and background events for Mark II $e^+e^-e^+e^-$, $e^+e^-\mu^+\mu^-$, and $\mu^+\mu^-\mu^+\mu^-$ final states for case (A) (pair masses $\geq 1\text{ GeV}/c^2$). Upper limits are at 95% C.L.

Data events	$e^+e^-e^+e^-$	$e^+e^-\mu^+\mu^-$	$\mu^+\mu^-\mu^+\mu^-$	Events failing lepton ID requirements
	10	10	1	17
Expected signal				
$e^+e^- \rightarrow e^+e^-e^+e^-$	10.9 ± 1.1			3.4 ± 0.4
$e^+e^- \rightarrow e^+e^-\mu^+\mu^-$		9.6 ± 1.1		7.0 ± 0.8
$e^+e^- \rightarrow \mu^+\mu^-\mu^+\mu^-$			0.76 ± 0.11	0.6 ± 0.08
Expected background				
$e^+e^- \rightarrow e^+e^-\tau^+\tau^-$	0.16 ± 0.06	0.09 ± 0.04	< 0.06	0.7 ± 0.1
$e^+e^- \rightarrow e^+e^-h^+h^-$	< 0.1	< 0.1	< 0.1	0.2 ± 0.1
$e^+e^- \rightarrow e^+e^-\gamma\gamma$	< 0.9			< 0.9
$e^+e^- \rightarrow \tau^+\tau^-$	< 1.2	< 1.2	< 1.2	1.2 ± 0.7
$e^+e^- \rightarrow q\bar{q}$	< 1	< 1	< 1	1.6 ± 0.7
Total	11.1	9.7	0.76	14.7
expected events	± 1.1 $+0.3$	± 1.1 ± 0.3	± 0.11 ± 0.02	± 1.4 ± 0.4

GeV/c².

We generated Monte Carlo events for each of the processes $e^+e^-e^+e^-$, $e^+e^-\mu^+\mu^-$, and $\mu^+\mu^-\mu^+\mu^-$ corresponding to the integrated luminosities of 6005 pb⁻¹, 3682 pb⁻¹, and 28 343 pb⁻¹, respectively.

The generated events were passed through a full detector simulation, which included the effects of multiple Coulomb scattering, photon conversions, electromagnetic interactions in the calorimeters, cell inefficiencies and dead wires in the drift chamber, tube inefficiencies and hadron punchthrough in the muon system. The simulated events were then passed through the same analysis code used for the real data analysis.

The number of events expected from Monte Carlo calculations were 10.9 ± 1.1 , 9.6 ± 1.1 , and 0.76 ± 0.11 for $e^+e^-e^+e^-$, $e^+e^-\mu^+\mu^-$, and $\mu^+\mu^-\mu^+\mu^-$, respectively, while 10, 10, and 1 events were observed in case (A). In case (B), the expected number of signal events were 14.0 ± 1.3 , 12.0 ± 1.3 , and 1.03 ± 0.13 for $e^+e^-e^+e^-$, $e^+e^-\mu^+\mu^-$, and $\mu^+\mu^-\mu^+\mu^-$, respectively, while 14, 13, and 1 events were observed. The errors given for the values predicted by the Monte Carlo calculations are statistical only.

In the data sample there was one $e^+e^-\mu^+\mu^-$ event with a photon of 1.5 GeV of energy which made an angle of 14.6° with the nearest track. This event cannot be compared separately with theory, since there is no complete QED calculation¹⁴ for the radiative corrections to order α^4 .

The emission of a real or virtual photon from the elec-

tron or positron before they annihilate can affect the observed cross section. We therefore estimated the correction to the four-lepton cross section for initial-state radiation. In our estimate we made use of the factorization of the infrared contributions and the strong peaking of the photon cross section in directions parallel to the motion of the charged particles. We used the probability function of Kuraev and Fadin¹⁵ to describe the emission of real photons. We generated four-electron events, which we simulated and passed through the same analysis programs as the real data, at various center-of-mass energies below 29 GeV. All appropriate kinematical transformations between the center-of-mass and the laboratory frames were taken into account. We found¹⁶ that the ratio of the cross section of $e^+e^- \rightarrow e^+e^-e^+e^-$ corrected for initial-state radiation to the lowest order (α^4) $e^+e^- \rightarrow e^+e^-e^+e^-$ cross section is 0.98 ± 0.08 , where the error is due to the limited Monte Carlo statistics.

Tables I and II show the predicted number of events from each of the previously mentioned background processes as well as the predicted number of events from the Monte Carlo calculation for cases (A) and (B), respectively.

The number of data events is presented without background subtraction. The number of expected data and background events have been corrected for the relative lepton identification efficiency of 0.97 ± 0.02 for electrons and muons in the data and the Monte Carlo simulations,¹⁷ and for initial-state radiation.

The errors attached to the predicted values (data and

TABLE II. Number of observed and expected signal and background events for Mark II $e^+e^-e^+e^-$, $e^+e^-\mu^+\mu^-$, and $\mu^+\mu^-\mu^+\mu^-$ final states for case (B) (pair masses ≥ 0.6 GeV/c²). Upper limits are at 95% C.L.

Data events	$e^+e^-e^+e^-$ 14	$e^+e^-\mu^+\mu^-$ 13	$\mu^+\mu^-\mu^+\mu^-$ 1	Events failing lepton ID requirements 37
Expected signal				
$e^+e^- \rightarrow e^+e^-e^+e^-$	14.0 ± 1.3			6.0 ± 0.7
$e^+e^- \rightarrow e^+e^-\mu^+\mu^-$		12.0 ± 1.3		11.1 ± 1.2
$e^+e^- \rightarrow \mu^+\mu^-\mu^+\mu^-$			1.03 ± 0.13	0.88 ± 0.11
Expected background				
$e^+e^- \rightarrow e^+e^-\tau^+\tau^-$	0.18 ± 0.06	0.09 ± 0.04	<0.06	1.0 ± 0.1
$e^+e^- \rightarrow e^+e^-h^+h^-$	<0.1	<0.1	<0.1	0.4 ± 0.1
$e^+e^- \rightarrow e^+e^-\gamma\gamma$	<0.9			<0.9
$e^+e^- \rightarrow \tau^+\tau^-$	<1.2	<1.2	<1.2	3.6 ± 1.2
$e^+e^- \rightarrow q\bar{q}$	<1	<1	<1	2.9 ± 1.0
Total expected events	14.2 ± 1.3 $+0.4$	12.1 ± 1.3 ± 0.4	1.03 ± 0.13 ± 0.03	25.9 ± 2.1 ± 0.8

background) are statistical, where the error on the correction for initial-state radiation has also been included. The errors in the total predicted events are statistical (first error) and systematic (second error). The systematic error consists of the errors on the number of events due to the relative particle-identification efficiencies in the data and the Monte Carlo simulations (2%) and the uncertainty in the integrated luminosity of the data (1.5%), added in quadrature.

The 95%-confidence-level (C.L.) upper limits are given in background processes where zero events passed the identification cuts.

We tested the sensitivity of our results to the identification cuts used. We define R_{tight} (R_{loose}) as the ratio of the observed data from all three processes ($e^+e^-e^+e^-$, $e^+e^-\mu^+\mu^-$, $\mu^+\mu^-\mu^+\mu^-$) to the number of corresponding predicted events, when tight (loose) identification cuts and the kinematical cuts of case (B) have been used. We define as loose identification cuts the ones used in the analyses previously presented, whereas tight identification cuts are defined as follows.

(i) An electron candidate in the liquid-argon calorimeter is tested with more restrictive criteria. This time, the electron identification requirement is essentially equivalent to an $E/P > 0.8$. Energy information from the end-cap shower counter is not used.

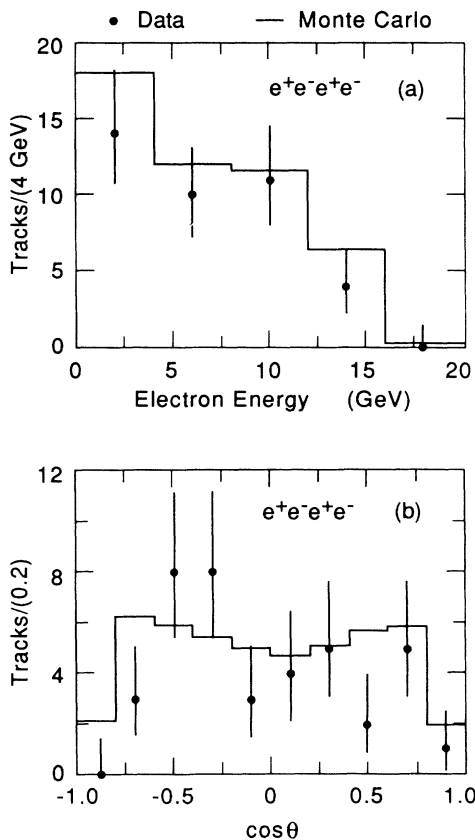


FIG. 3. Distribution of electrons (e^\pm) in $e^+e^-e^+e^-$ events: (a) electron energy; (b) $\cos(\theta)$. The histogram is the QED prediction to order α^4 .

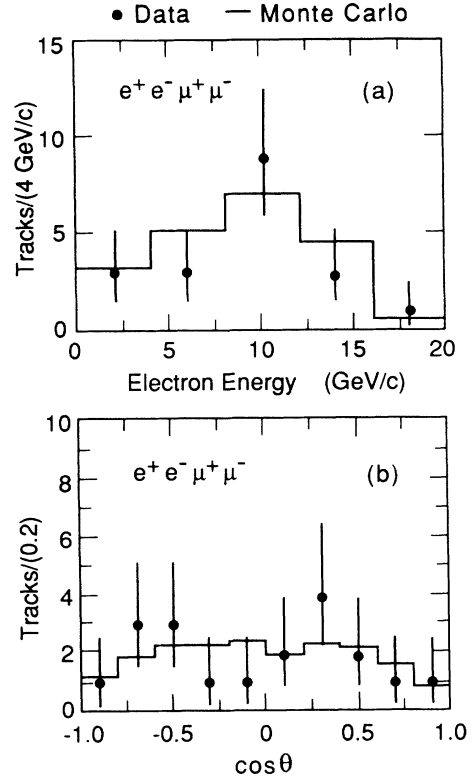


FIG. 4. Distribution of electrons (e^\pm) in $e^+e^-\mu^+\mu^-$ events: (a) electron energy; (b) $\cos(\theta)$. The histogram is the QED prediction to order α^4 .

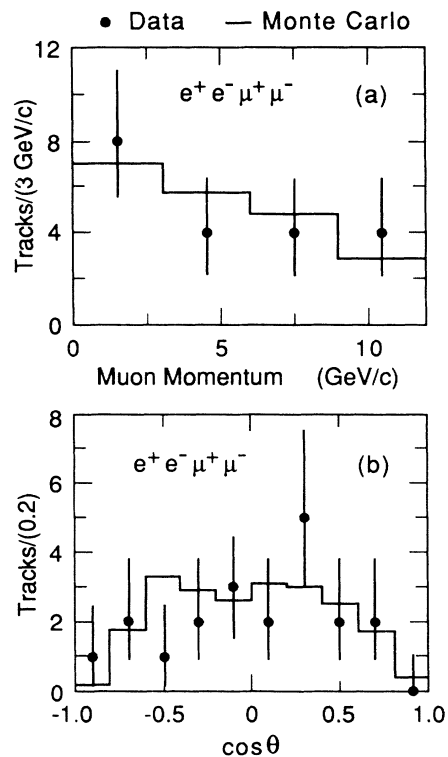


FIG. 5. Distribution of muons (μ^\pm) in $e^+e^-\mu^+\mu^-$ events: (a) muon momentum; (b) $\cos(\theta)$. The histogram is the QED prediction to order α^4 .

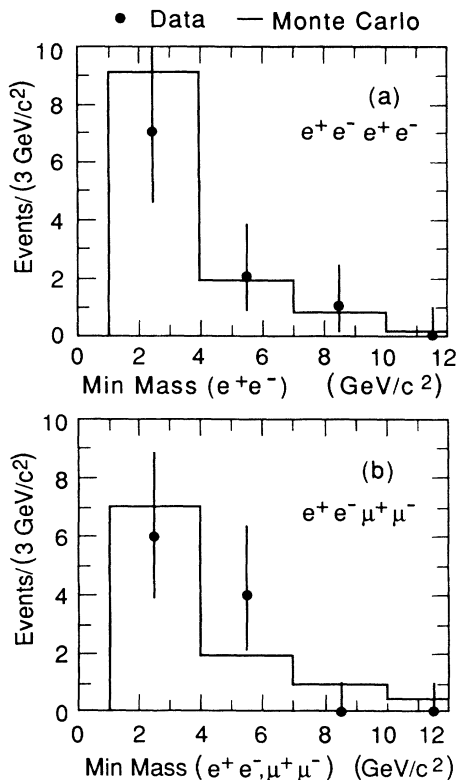


FIG. 6. Lowest-invariant-mass distribution in (a) $e^+e^-e^+e^-$ events; (b) $e^+e^-\mu^+\mu^-$ events. The histogram is the QED prediction to order α^4 .

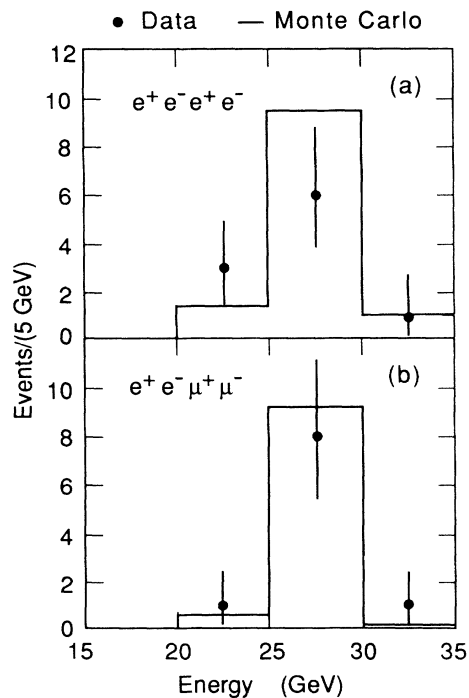


FIG. 7. Energy distribution in (a) $e^+e^-e^+e^-$ events; (b) $e^+e^-\mu^+\mu^-$ events. The histogram is the QED prediction to order α^4 .

(ii) A muon candidate is required to leave hits in either the first three or all four layers of the muon system consistent with its expected range and track extrapolation error.

We observed a total of 28 events from the three processes when loose identification cuts were used, and found $R_{\text{loose}} = 1.04 \pm 0.20$. When tight identification cuts were used we observed a total of 18 events from the three processes and found $R_{\text{tight}} = 0.96 \pm 0.23$. Their difference, $R_{\text{loose}} - R_{\text{tight}} = 0.08 \pm 0.14$, where the errors are statistical only, is an indication that the results of this analysis do not depend on the details of the lepton identification criteria.

Various distributions are shown for the final samples and compared with QED calculations for case (A) normalized to the experimental integrated luminosity of 205 pb^{-1} . These distributions include all four tracks of an

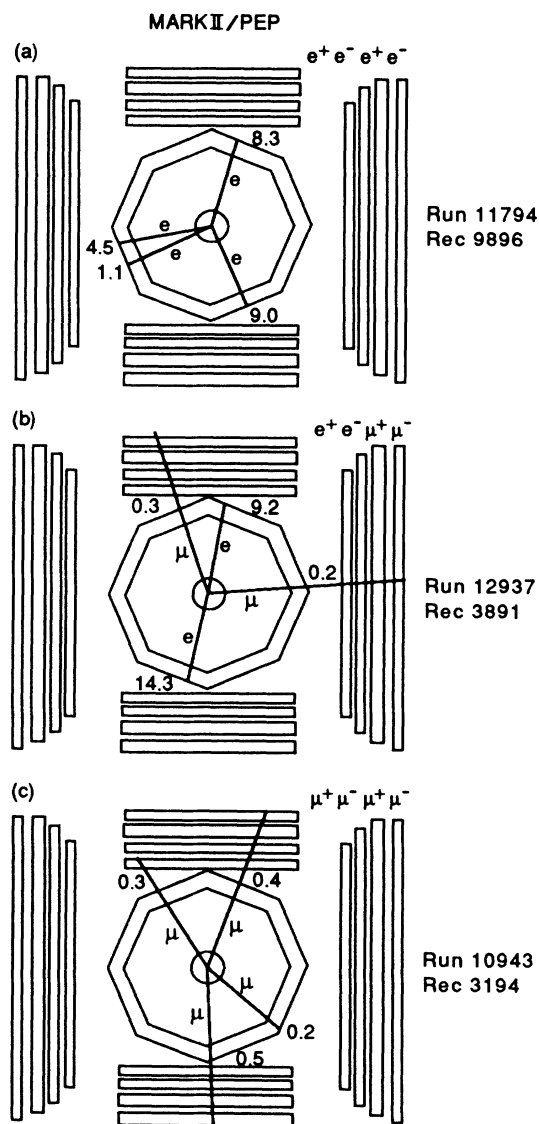


FIG. 8. Characteristic event pictures of $e^+e^-e^+e^-$, $e^+e^-\mu^+\mu^-$, and $\mu^+\mu^-\mu^+\mu^-$ final states, observed in the data.

identified event, even when only three tracks, or two tracks of the same charge sign have been individually identified. In such cases, the assumption of lepton-number conservation determines the identity of the remaining tracks in the event. Figures 3 and 4 show the energy and angular distribution of electrons (e^\pm) in $e^+e^-e^+e^-$ and $e^+e^-\mu^+\mu^-$ events, whereas Fig. 5 shows the momentum and angular distribution of muons (μ^\pm) in $e^+e^-\mu^+\mu^-$ events. Figure 6 shows the minimum mass distribution of two leptons. Here we took the lowest invariant mass of all four possible combinations (e^+e^-) in $e^+e^-e^+e^-$ events, and the lower invariant mass of the e^+e^- or $\mu^+\mu^-$ combinations in $e^+e^-\mu^+\mu^-$ events. Figure 7 shows the energy distribution in $e^+e^-e^+e^-$ (a) and $e^+e^-\mu^+\mu^-$ (b) events. They all agree well with the QED predictions. Finally, Fig. 8 shows characteristic event pictures for each of the three processes $e^+e^-e^+e^-$, $e^+e^-\mu^+\mu^-$, and $\mu^+\mu^-\mu^+\mu^-$.

Taking into account the acceptance of the Mark II detector, the selection criteria applied to the data, the total integrated luminosity of the examined data sample, we find agreement between our results and those from other experiments (Refs. 5 and 7). We, too, do not observe any

deviation from the QED expectations to order α^4 . A recent analysis of HRS PEP data,¹⁸ presented in a companion paper, also confirms agreement with QED.

D. Conclusions

Four-lepton final states in e^+e^- interactions were studied using the Mark II detector at PEP. Data for $e^+e^- \rightarrow e^+e^-e^+e^-$, $e^+e^- \rightarrow e^+e^-\mu^+\mu^-$, and $e^+e^- \rightarrow \mu^+\mu^-\mu^+\mu^-$ processes were compared to the QED Monte Carlo calculation of Berends *et al.* The experimental results are in good agreement with the theoretical predictions of QED to order α^4 .

ACKNOWLEDGMENTS

One of the authors (M.P.) would like to thank C. Hawkins and D. Stoker for very many useful discussions. This work was supported in part by the U.S. Department of Energy under Contracts Nos. DE-AC03-76SF00098 (Lawrence Berkeley Laboratory), DE-AC02-76ER03064 (Harvard University), DE-AC02-76ER01112 (University of Michigan), and DE-AC03-76SF00515 (SLAC).

^(a)Present address: Brookhaven National Laboratory, Upton, NY 11973.

^(b)Present address: Boston University, Boston, MA 02215.

^(c)Present address: Carleton University, Ottawa, Ontario, Canada K1S 5B6.

^(d)Present address: California Institute of Technology, Pasadena, CA 91125.

^(e)Present address: CERN, CH-1211, Genève 23, Switzerland.

^(f)Present address: University of California, Riverside, CA 92521.

^(g)Present address: University of California, Santa Cruz, CA 95064.

^(h)Present address: University of Chicago, Chicago, IL 60637.

⁽ⁱ⁾Present address: Columbia University, New York, NY 10027.

^(j)Present address: University of Florida, Gainesville, FL 32611.

^(k)Present address: Fermilab, Batavia, IL 60510.

^(l)Present address: Université de Genève, CH-1211, Genève 4, Switzerland.

^(m)Present address: Harvard University, Cambridge, MA 02138.

⁽ⁿ⁾Present address: University of Illinois at Urbana-Champaign, Urbana, IL 61801.

^(o)Present address: Lawrence Berkeley Laboratory, University of California, Berkeley, CA 94720.

^(p)Present address: University of Oklahoma, Norman, OK 73019.

^(q)Present address: University of Pennsylvania, Philadelphia, PA 19104.

^(r)Present address: Stanford Linear Accelerator Center, Stanford, CA 94309

^(s)Present address: University of Wisconsin, Madison, WI 53706.

¹T. Kinoshita, Report No. CERN-TH-5097/88, 1988 (unpublished).

²A. S. Elkovskii, Novosibirsk Institute of Nuclear Physics, Academy of Sciences Report No. 88-050, 1988 (unpublished).

³A. Davies and S. Brodsky, Report No. SLAC-PUB-4498, 1987

(unpublished); J. Grifols and A. Mendez, Phys. Rev. D **26**, 1809 (1982); A. Mendez and F. Orteu, Phys. Lett. **163B**, 167 (1985), and references therein. A general review of recent studies beyond the standard model can be found in *Lepton and Photon Interactions*, proceedings of the International Symposium on Lepton and Photon Interactions at High Energies, Hamburg, West Germany, 1987, edited by R. Rückl and W. Bartel [Nucl. Phys. B (Proc. Suppl.) **3** (1987)].

⁴F. A. Berends, P. Daverveldt, and R. Kleiss, Nucl. Phys. **B239**, 395 (1984); **B253**, 441 (1985); **B264**, 265 (1986).

⁵Mark J Collaboration, Report No. DESY-85-073, 1985 (unpublished); JADE Collaboration, Z. Phys. C **30**, 545 (1986); ASP Collaboration, SLAC-Report-337, 1989 (unpublished).

⁶CELLO Collaboration, Report No. DESY-84-103, 1984 (unpublished).

⁷CELLO Collaboration, Z. Phys. C **43**, 1 (1989).

⁸R. H. Schindler *et al.*, Phys. Rev. D **24**, 78 (1981); J. Jaros, in *Proceedings of the International Conference on Instrumentation for Colliding Beam Physics*, Stanford, California, 1982, edited by W. W. Ash (SLAC Report No. 250, Stanford, 1982).

⁹The end-cap shower counters covered the forward and backward regions of Mark II. They consisted of two sheets of lead, each one 2.3-radiation-lengths thick, alternating with two layers of proportional wire chambers. They measured electromagnetic showers between the polar angles of 15° and 40° , over most of the azimuthal range. The energy resolution of the end-cap system was $50\%/\sqrt{E}$, for photons and electrons, where E is in GeV. This resolution proved sufficient for discriminating electrons from muons in the end-cap region [M. Petradza, Ph.D. thesis, University of Michigan, SLAC-Report-347, 1989 (unpublished); Petradza and Lüth, Mark II/SLC note 252].

¹⁰M. E. Nelson, Ph.D. thesis, Lawrence Berkeley Laboratory Report No. LBL-16724, 1983.

¹¹T. Sjostrand, Comput. Phys. Commun. **39**, 347 (1986).

¹²C. Peterson *et al.*, Phys. Rev. D **27**, 105 (1983).

- ¹³CALCUL Collaboration, F. A. Berends *et al.*, Nucl. Phys. **B239**, 395 (1984), calculation of the matrix elements of the process; Monte Carlo program, ASP Collaboration, C. Hawkins, Ph.D. thesis, Stanford University, SLAC-Report-337, 1989 (unpublished).
- ¹⁴F. A. Berends, P. Daverveldt, and R. Kleiss, Nucl. Phys. **B253**, 421 (1985); Comput. Phys. Commun. **40**, 271 (1986). They only considered the radiative corrections of multiperipheral four-lepton production which peaks at small angles.
- ¹⁵E. A. Kuraev and V. S. Fadin, Yad. Fiz. **41**, 733 (1985) [Sov. J. Nucl. Phys. **41**, 466 (1985)].
- ¹⁶Petradza (Ref. 9).
- ¹⁷P. R. Burchat, Ph.D. thesis, Stanford University, SLAC-Report-292, 1986 (unpublished).
- ¹⁸M. Petradza *et al.*, following paper, Phys. Rev. D **42**, 2180 (1990).